Characterization of an Organic Field-Effect Thin-Film Transistor in Operation Using Fluorescence-Yield X-Ray Absorption Spectroscopy

Hiroyuki S. Kato,[1] Hiroyuki Yamane,[2] Nobuhiro Kosugi,[2] and Maki Kawai[1,3]

[1]*RIKEN (The Institute of Physical and Chemical Research), Wako, Saitama 351-0198, Japan*
[2]*Institute for Molecular Science and the Graduate University for Advanced Studies, Okazaki, Aichi 444-8585, Japan*
[3]*Department of Advanced Materials Science, University of Tokyo, Kashiwa, Chiba 277-8501, Japan*
(Received 6 December 2010; published 30 September 2011)

In situ element-specific observation of electronic states of organic films beneath metal electrodes is achieved by x-ray absorption spectroscopy (XAS) in the bulk-sensitive fluorescence-yield (FY) mode. The molecular orientation in Au-covered oligo-thiophene films is confirmed by the C K-edge FY-XAS spectra and the applied bias dependence of the spectra is successfully detected for the first time. The present method can give deeper insights into the electronic-state investigation of various real-device systems under operational conditions.

Recent progress in molecular devices is rapidly making this field a promising candidate for the next-generation nanoelectronics. However, even in the case of archetypal organic field-effect transistors (OFETs) [1–3], it is not clear whether or not the energy diagram of OFETs is the same as that of inorganic semiconductors, i.e., a conductive channel creation by band bending of the semiconductor energy levels in a metal-insulator-semiconductor (MIS) structure. Therefore, precise characterization of electronic states in organic thin-film devices has been required under operational conditions.

For the *in situ* observation of molecular electronic states, several photon-in-photon-out experiments have been attempted, because of little perturbation to the detection even under an applied electric field [4–13]. Photoabsorption spectroscopy between ultraviolet (UV) and near infrared (NIR) rays is often used to characterize OFETs [4–8]. Such measurements have focused on the electron transition at the band gap of organic films, and disclosed new electronic states created by field-induced carriers into the films, as polaron (or bipolaron) midgap states observed in conductive polymers [5–8]. This energy diagram clearly differs from that of the conventional band bending model in inorganic FETs. In addition, the studies using infrared (IR) vibrational spectroscopy [8–10] have shown a spectral change depending on applied bias, and claimed the creation of ionic species originated from the field-induced carriers in the organic films, from consistent observations of polaron states.

In contrast to the above-mentioned spectroscopic approaches, nonlinear optical spectroscopy such as sum-frequency generation (SFG) [11] and second-harmonic generation (SHG) [12,13] has revealed different characteristics of OFETs. The SFG measurement detects the vibration spectral change of non-π-conjugated parts in molecules, corresponding to the number of active carriers [11]. Since the induced charge concentrates into the

π states near the Fermi level in organic molecules, the SFG results are important in considering noncharged parts in the thin films. In addition, the SHG measurement is sensitive to a local electric field in organic films in OFET, and shows a two-dimensional distribution of the field which is consistent with the electric field distributions expected from the typical MIS model of FET [12,13]. To describe the energy diagram of OFETs, further investigation is necessary.

In this study, to elucidate *in situ* electronic states of OFETs under operational conditions, we utilize x-ray absorption spectroscopy (XAS) in the bulk-sensitive fluorescence-yield (FY) mode, which is a type of photon-in-photon-out measurement. In the measurement, electrons in the core level are excited to unoccupied states as a function of x-ray photon energy; thus, the spectra of a near-edge x-ray absorption fine structure (NEXAFS) are obtained at the specific sites of selected elements included in target molecules. The XAS measurement using soft x rays is often performed in the electron-yield (EY) detection mode, because most inner-shell excited states are nonradiatively deexcited by emitted electrons through Auger or Auger-like decay processes and other secondary processes. However, the mean free path of emitted electrons is too short to observe the inner electronic states of organic thin films. In contrast, the fluorescent x rays have a long penetration depth (> 100 nm) [14–21]. FY-XAS is a promising element-specific method for detecting the inner electronic states of organic thin films [22], even beneath thin metal electrodes [23]. Recently, fuel cells under the bias voltage have been investigated [24,25], using the deeper x rays above ≈ 10 keV with longer penetration depth and ability to excite heavy elements under quasiambient conditions. In contrast to that, the soft x rays are essential for the investigation of organic thin-film devices consisting of light elements, such as C, N, and O atoms. To the best of our knowledge, this is the first report on the

successful FY-XAS study of characteristics of organic devices under operational conditions.

Figure 1 shows schematic views of an organic thin film and a highly efficient fluorescence detection system used in the present study, and observed FY-XAS spectra of the organic thin-film. For OFETs, poly- and oligo-thiophene show high performance in terms of the *p*-type-like electric property [1–3,5–11]. α, ω-Dihexylsexithiophene (DH6T) [Fig. 1(a)] is a typical oligo-thiophene, and easily forms well-ordered thin films, as shown in Fig. 1(b) [26,27]. We fabricated DH6T thin films (17 nm thick corresponding to the 4–5 monolayers) on SiO_2 (500 nm thick)-precovered Si substrates (highly B-doped, 0.5 mm thick), hereafter SiO_2/Si. We confirmed a clear step-and-terrace morphology of the films by atomic force microscopy (AFM). For the measurement of bias dependence, a full-covered top-contact Au electrode (25 nm thick) was deposited on the DH6T thin films while cooling the substrate below 20 °C. This electrode structure is different from that of a normal OFET; i.e., there is no separation between the source and drain electrodes, but is helpful for understanding the observed field effects because of the uniformity of the field in the films.

The FY-XAS measurement was performed at the beam line BL3U of the UVSOR facility in IMS. The samples were set in a BL3U end station through the sample entry system. The fluorescence signals were simply detected using a retarding-field detector consisting of microchannel plates (MCPs) in the counting mode. To accumulate weak signals, a center-hole-type MCP was used, in which incident x rays passed through the center hole and fluorescence x-ray signals were effectively detected at a wide acceptance angle, as shown in Fig. 1(c). For the characterization of DH6T-FET, C *K*-edge spectra were measured with an x-ray energy resolution of 50 meV at 290 eV. Through these measurements, the applied retarding bias exceeded -1 kV to repel photoelectrons excited by not only fundamental x rays but also higher-order x rays generated by the monochromator at BL-3U. The absolute photon energy was calibrated by measuring the C *K*-edge XAS spectra of HOPG, for Ref. [28].

Figure 1(d) shows the incident angle dependence of the FY-XAS spectra of the Au-covered DH6T thin film. In the measurement, the sample was rotated horizontally in the plane including linearly polarized x rays [Fig. 1(c)]. Since the observed spectra had an influence of the carbide contamination on the beam line and the samples, the spectra were corrected using the mesh current monitoring the incident x-ray intensity and the spectra of Au-covered SiO_2/Si substrates measured in the same condition [29]. The corrected spectra were normalized in intensity using the post-edge signal height at 320 eV. The spectra are very close to the previously reported EY-XAS spectra of α, ω-dipropenesexithiophene thin films [30]: two sharp $\pi^*_{C=C}$ resonant peaks near 285 eV, a sharp $\sigma^*_{C-S/C-H}$ resonant peak overlapping at 287.4 eV, and two or more broad σ^*_{C-C} resonant peaks between 292 and 304 eV. The incident angle dependence reflecting the molecular orientation is also consistent with the expected ordered structure [Fig. 1(b)] [26,30]. In comparison with the $\sigma^*_{C-S/C-H}$ peak height, the relative intensity of the $\pi^*_{C=C}$ peaks decreases with increasing the incident angle, while that of the σ^*_{C-C} peaks increases. These results clearly show that the FY-XAS measurement can reveal easily the inner electronic states of organic thin films and its averaged molecular orientation even beneath Au electrodes. As a result, it is directly shown that the molecular orientation in the films is not significantly perturbed by our electrode deposition procedure.

Figure 2 shows successfully observed FY-XAS spectra of the Au-covered DH6T film under an applied bias, using the highly efficient fluorescence detection system shown in Fig. 1(c). The field effects in the DH6T films were measured at the normal incidence. The gate bias (V_G) was
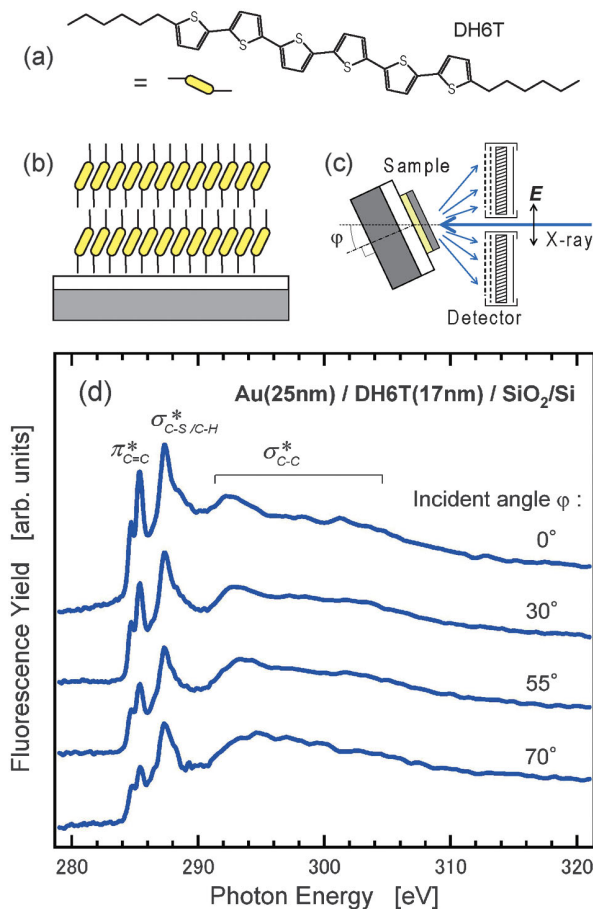

FIG. 1 (color). Structural chemical formula of α, ω-dihexylsexithiophene (DH6T) (a) and its schematic crystal structure on substrate (b). A sketch of the FY-XAS measurement system is also shown in (c). Incident angle dependence of C *K*-edge XAS spectra of Au-covered DH6T thin films on SiO_2/Si substrate (d), in which the thicknesses of Au, DH6T, and SiO_2 were 25, 17, and 500 nm, respectively.
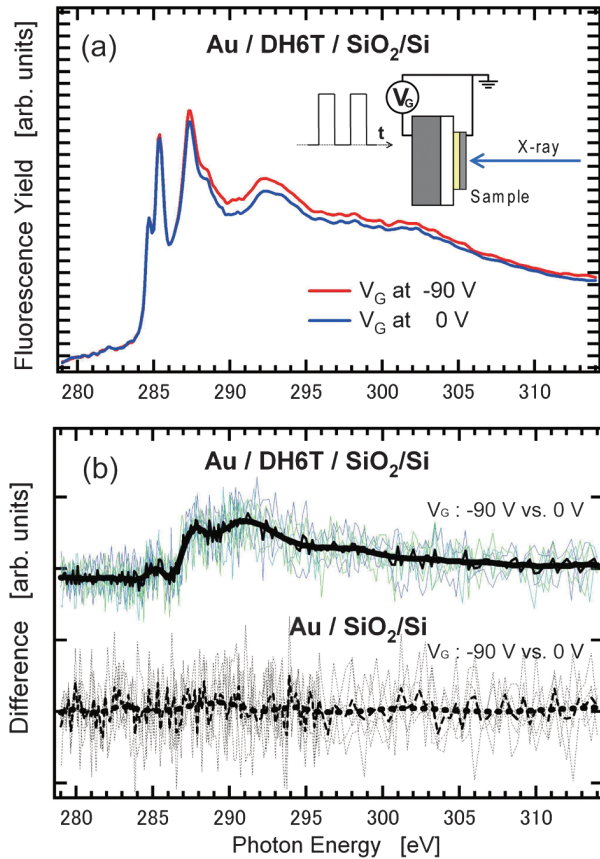
FIG. 2 (color).   Bias dependence of FY-XAS spectra of Au-covered DH6T thin-film (a). The gate bias V_G was applied as a square wave (7 Hz) to the highly doped Si substrate while electrically earthing the top Au electrode (inset). Then, the spectra at biases of 0 V and -90 V were obtained, simultaneously, as shown in (a). Their spectral difference was plotted using solid lines on the upper side in (b). For comparison, the difference spectra of the non-DH6T sample were also plotted using broken lines on the lower side in (b). In (b), thin, middle, and bold lines indicate raw spectra in one scan, an averaged spectrum, and a numerically smoothed spectrum of an averaged spectrum, respectively.

applied to the highly doped Si substrate, and the top Au electrode was electrically grounded [Fig. 2(a), inset]. Note that, the V_G was applied as a square wave (7 Hz) synchronized to two signal counters for each of the top and bottom bias levels, which enabled us to get two different bias spectra in one photon energy sweep and to compare details of their spectra with sufficient reliability. Figures 2(a) and 2(b) show the FY-XAS spectra under the V_G-on/off conditions and their difference spectra, respectively. For the acquisition of the spectra, signals were accumulated for 3 sec at each point in the spectrum. The observed spectra were treated by the spectral correction procedure, as mentioned above [29], and more than six spectra were averaged to obtain the reliable spectra at each bias voltage. A significant difference between the spectra was detected successfully. The feature of the difference

spectrum differs from the original DH6T spectrum: small peaks near 285 eV, a sharp peak at 287.8 eV, and a broad peak at 291 eV. When the organic layer was not deposited on the substrate, i.e., Au-covered SiO_2/Si sample, of course, no meaningful signals were detected, as shown in Fig. 2(b) (dashed lines in the lower spectra). Although, depending on the gate bias voltage, a tiny unfavorable signals possibly due to elusive electrons were detected, the signals had a flat feature, i.e., just an offset, on the difference spectrum of the Au-covered SiO_2/Si samples, as shown in Fig. 2(b). We are, therefore, confident that the obtained difference spectra of the DH6T samples reflect the field effect in the DH6T films, without spurious signals.

Figure 3(a) shows the V_G dependence of the FY-XAS spectral difference of the DH6T film, in which a gradual change was observed. At the negative V_G, the difference spectrum increased its intensity with increasing the bias amplitude. The shape of the spectra slightly differed between the smaller and larger bias amplitudes; the shape was like a step function at a small amplitude cf. $V_G =$ -20 V vs 0 V, and then the peaks at 287.8 and 291 eV became clearer at the larger amplitude. In contrast to that, at a positive V_G, the V_G dependence shows an opposite feature in the spectral intensity; that is, some part of the signals became smaller with increasing the amplitude of positive bias than those observed in the nonbiased spectra. The spectral evolutions, however, seem to be the same in shape. Consequently, the spectral changes at the positive and negative V_G are almost antisymmetric.

Figure 3(b) shows relative changes (%) of the difference spectra [Fig. 3(a)] at fixed incident photon energies of 292 eV (near the K-edge) and 304 eV (the post-edge) in comparison to the offset measured at 280 eV. Since the photon energy was fixed, the total accumulation time at each plot could set long enough by a factor of about 20, i.e., 440 s, compared to that at the spectral measurements, and the detailed bias dependence could be acquired. The intensity change was continuous in the whole bias range and to be antisymmetric depending on the applied bias voltage, while the change is not linear to the bias, and not uniform.

According to previous studies using photoabsorption spectroscopy [5–8], field-induced carriers have a possibility to influence the FY-XAS spectra. If this is the case, the induced carriers would affect the electronic states near the Fermi level, as reported [5–8]. However, the observed spectral difference shows only a small change at the $\pi^*_{C=C}$ resonant peaks near 285 eV. In addition, since oligo-thiophene thin films have p-type-like electric properties in OFET devices [1–3,5–11], the spectral change has been mainly expected at the negative V_G. This is also inconsistent with our observation. The effect of induced carriers can be minor in the FY-XAS spectra in the present system. The observed continuous and antisymmetric intensity change, shown in Fig. 3, indicates that the observed bias dependence in the XAS spectra dose not originate
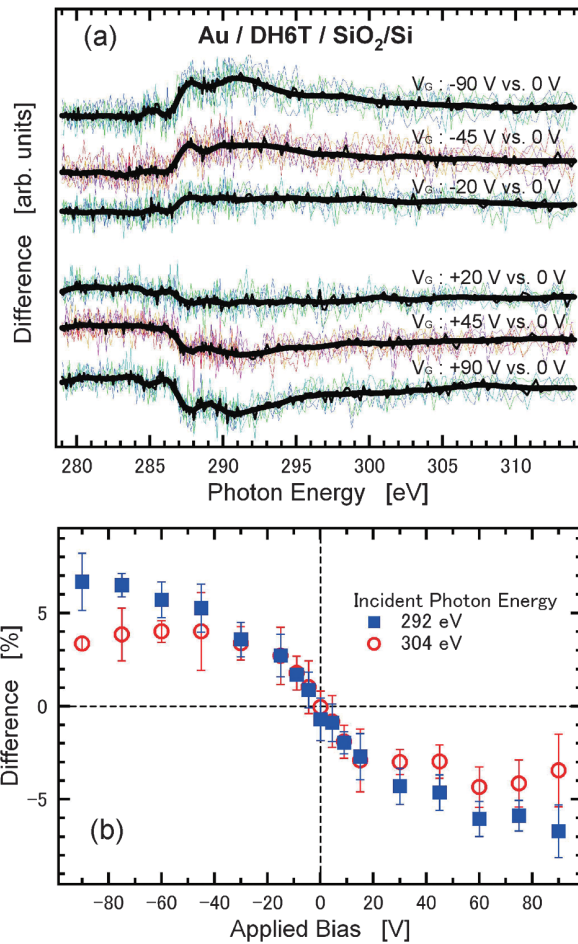
FIG. 3 (color). Bias dependence of the FY-XAS spectral difference (a) and the intensity difference at fixed incident photon energies (b), as a function of the applied bias: In Fig. 3(a), the measurement parameters, the signal correction procedure, and the kinds of the plotted lines are the same to those of Fig. 2(b). For Fig. 3(b), the FY-XAS intensity difference was observed at the photon energies at 292 and 304 eV in comparison to the offset measured at 280 eV with the same measurement parameters at Fig. 3(a), except the fixed photon energies and a longer total accumulation time (see text).

from any discontinuous phenomena, such as carrier injection, but results from some continuous modification of the molecular state by the applied electric field.

Details of the intra- and/or intermolecular state modification by the electric field cannot be defined within the present work. Under the electric field, several modifications in the molecular film are expected: for instance, geometrical change, polarization, and band-bending-like distortion of the electric states. At the DH6T films, a definite static dipole is not expected, because of the symmetrical structure of the DH6T molecule. Only the induced polarization and its molecular dipole should respond to the electric field. Since the induced dipole always appears giving attractive polarity, it may lead the longer molecular axis to arrange parallel to the line of electric force at both

positive and negative biases. However, this kind of geometrical change of the molecules cannot explain the observed antisymmetric change of the spectra. While such a geometrical change may induce a certain intensity change of the π^* peaks near 285 eV, in addition, it was hardly detected in Fig. 3(a).

The induced molecular polarization is also a candidate for the origin of the spectral change, itself. When the polarization is induced, both occupied and unoccupied molecular orbitals near the Fermi level should suffer a change depending on the electric field. As a result, the polarization should provide both decrease and increase of some components in the XAS spectra reflecting on the overlap modification of the respective core and unoccupied states. However, the observed spectral changes differ from such simple expectation. Of course, a possibility of composite factors, such as a polarization accompanied with structural modification in the molecules, cannot be denied. In addition, the contribution of a band-bending-like distortion in the intermolecular interaction of the electric states is conceivable. Since the band bending in organic films is a consequence of the collective polarization of the molecules in the films, i.e., dielectric property, which might occur in OFET [12,13,31], every electric states shift keeping the same separation in energy. In this simple description, therefore, the spectral change could not be expected under any V_G. At the interface between the organic film and the insulator, however, the energy band should shift upward and downward depending on the negative and positive V_G, respectively, and thus the potential well of molecules at the interface becomes shallower and deeper. If such potential modification could affect to the XAS spectra, the observed antisymmetric change depending on V_G is possibly explained well. For this argument, further systematic experiments and careful analysis are required.

Finally, we consider the features of the difference spectra, i.e., two peaks at 287.8 and 291 eV observed at the higher applied bias. Since the spectral change originates from the electric field rather than the induced carriers, the difference spectra may reflect a part sensitive to the field in the film. In this aspect, it is interesting that the observed two peaks and the entire shape are more similar to the peaks at 288 and 291.5 eV observed in the oriented hexanethiolate monolayer on Cu(111) at the normal incidence [32] than the peaks in the original DH6T spectra. These results suggested that the hexyl groups selectively suffer from the field effects in DH6T, and lead us to conclude that the distribution of the electric field is not uniform in the DH6T thin film. Although there are several studies of the electric field distribution in OFET by microscopic SHG [12,13] and Kelvin probe force microscopy (KFM) [31] on the submicron scale, there is not yet any experimental study of the electric field distribution on the molecular scale. Since precise knowledge of the field effects on

intramolecular states are indispensable for developing future single-molecular devices, more diversified arguments about the observed FY-XAS profile change should be important.

In summary, the electronic states of organic thin-film devices were studied using FY-XAS. *In situ* element-specific observation of hidden electronic states of DH6T films beneath Au electrodes was achieved even under operational conditions. In fact, the molecular orientation in the Au-deposited films was clearly confirmed by the C *K*-edge FY-XAS measurements. Moreover, the bias dependence of the FY-XAS spectra of DH6T films was successfully detected, in which the origin of the spectral change is considered to be a molecular state modification by the applied electric field. The feature of difference spectra in the bias dependence suggested that the applied electric field is not uniform in the DH6T films. This method has many advantages to observe the inner part of heterogeneous thin films and thus will be utilized for characterizing various organic thin-film devices.

[1] A. Tsumura *et al.*, Appl. Phys. Lett. **49**, 1210 (1986).
[2] H. E. Katz, Chem. Mater. **16**, 4748 (2004).
[3] A. Facchetti, Mater. Today **10**, 28 (2007).
[4] J. H. Burroughes *et al.*, Nature (London) **335**, 137 (1988).
[5] K. E. Ziemelis *et al.*, Phys. Rev. Lett. **66**, 2231 (1991).
[6] H. Sirringhous *et al.*, Nature (London) **401**, 685 (1999).
[7] P. J. Brown *et al.*, Phys. Rev. B **63**, 125204 (2001).
[8] Z. Q. Li *et al.*, Nano Lett. **6**, 224 (2006).
[9] Y. Furukawa, Macromol. Symp. **205**, 9 (2004).
[10] L. G. Kaake *et al.*, J. Am. Chem. Soc. **129**, 7824 (2007).
[11] H. Ye *et al.*, J. Am. Chem. Soc. **128**, 6528 (2006).
[12] T. Manaka *et al.*, Appl. Phys. Lett. **89**, 072113 (2006).
[13] T. Manaka *et al.*, Nat. Photon. **1**, 581 (2007).
[14] D. A. Fischer *et al.*, Rev. Sci. Instrum. **60**, 1596 (1989).
[15] C. Y. Yang *et al.*, Phys. Rev. B **42**, 2231 (1990).
[16] D. A. Fischer *et al.*, Phys. Rev. B **44**, 1427 (1991).
[17] G. P. Hastie *et al.*, J. Chem. Soc., Faraday Trans. **92**, 783 (1996).
[18] D. A. Fischer *et al.*, Appl. Surf. Sci. **133**, 58 (1998).
[19] A. Agui *et al.*, Phys. Rev. B **59**, 10792 (1999).
[20] G. D. Meitzner and D. A. Fischer, Microchem. J. **71**, 281 (2002).
[21] Ph. Wernet *et al.*, Science **304**, 995 (2004).
[22] C. Hub *et al.*, J. Mater. Chem. **20**, 4884 (2010).
[23] H. S. Kato *et al.*, J. Electron Spectrosc. Relat. Phenom. **174**, 93 (2009).
[24] M. Tada *et al.*, Angew. Chem., Int. Ed. **46**, 4310 (2007).
[25] E. Principi *et al.*, J. Synchrotron Radiat. **14**, 276 (2007).
[26] F. Garnier *et al.*, J. Am. Chem. Soc. **115**, 8716 (1993).
[27] M. Kakita and H. Tada, Mol. Cryst. Liq. Cryst. **471**, 229 (2007).
[28] F. Atamny *et al.*, J. Phys. Chem. **96**, 4522 (1992).
[29] See Supplemental Material at http://link.aps.org/supplemental/10.1103/PhysRevLett.107.147401 for details of the spectral correction procedure.
[30] D. M. DeLongchamp *et al.*, Adv. Mater. **17**, 2340 (2005).
[31] S. Ikeda *et al.*, J. Appl. Phys. **101**, 094509 (2007).
[32] H. Kondoh *et al.*, J. Phys. Chem. B **108**, 12946 (2004).